Materials Physics and Mechanics 39 (2018) 27-34 Received: November 1, 2017

AB INITIO SIMULATION OF GRAPHENE INTERACTION WITH SiO_2 SUBSTRATE FOR NANOELECTRONICS APPLICATION

Dzmitry Hvazdouski*, Viktor Stempitsky

Belarusian State University of Informatics and Radioelectronics, Minsk, Belarus

*e-mail: gvozdovsky@bsuir.by

Abstract. First-principles calculations were carried out by the Vienna Ab initio Simulation Package (VASP). Preliminary calculations showed that DFT-D3 method with Becke-Jonson damping present good agreement of lattice constant with experiment data. Ground state of graphene position on the SiO_2 surfaces obtained has been determined. Interlayer distances between graphene and different types of quartz substrate have been calculated; the interlayer distances being 3.31 Å and 4.32 Å for models with open oxygen dangling bonds and with open silicon dangling bonds, respectively. The adsorption energy of graphene on the amorphous SiO_2 surface with open oxygen dangling bonds is larger than the adsorption energy on the second type of surface. We observed the 0.12 eV band gap in the case with open oxygen dangling bonds. This kind of quartz surface can be source of a charge puddle.
Keywords: ab initio calculation, adsorption, amorphous SiO_2, graphene, surface

1. Introduction

Graphene is a promising material with high charge mobility [1−3]. The substrate material has a significant negative influence on graphene charge carrier mobility. Quartz is well established as a substrate in graphene technology. However, the mobility of charge carriers in such systems is worse than the theoretical calculations for a pure graphene sheet [2, 3]. The space charge inhomogeneity (so-called charge puddle) leads to degradation of graphene electronic properties [4−6]. Physical characteristics leading to the occurrence of electron-hole puddles are not identified uniquely [1, 4, 7]. Possible reasons for their formation are: open dangling bonds [8], point defects in the graphene layer [9−11], and charged impurities [12, 13]. The results of experimental work [14] prove that the presence of dangling bonds on the surface of a SiO_2 quartz substrate during the device fabrication may be the main reason for the occurrence of an electron-hole puddle in graphene.

Amorphous SiO_2 has various types of surface species. In this study the impact of amorphous SiO_2 surface variety on the structure and electronic properties of graphene has been investigated. The α-quartz is the most stable polymorphic modification of SiO_2, and its most stable surface is (001) [15, 16]. Fig. 1 shows the elementary cells of graphite and α-SiO_2. Two typical quartz substrates were chosen for modeling: oxygen atoms are on the surface (O^{unsat}), and silicon atoms are on the surface (Si^{unsat}). Besides the similar substrates were modeled, but already passivated by hydrogen atoms: O^{sat} and Si^{sat}.

It is possible to passivate the broken bonds with hydrogen atoms absorbed by the substrate surface for each type of bonds (Si^{sat} and O^{sat}). In Ref. [17] it was found that the most stable surface of α-SiO_2 has the atomic configuration (0001) (O^{sat}). However the calculations were performed by quantum-mechanical simulation without taking into account van der Waals forces which are significant in layered structures. For this reason, the quantum-

http://dx.doi.org/10.18720/MPM.3912018_5

mechanical study of a graphene monolayer deposited on all four types of surfaces: O^{unsat}, O^{sat}, Si^{unsat} and Si^{sat} that takes into account van der Waals forces is of interest.

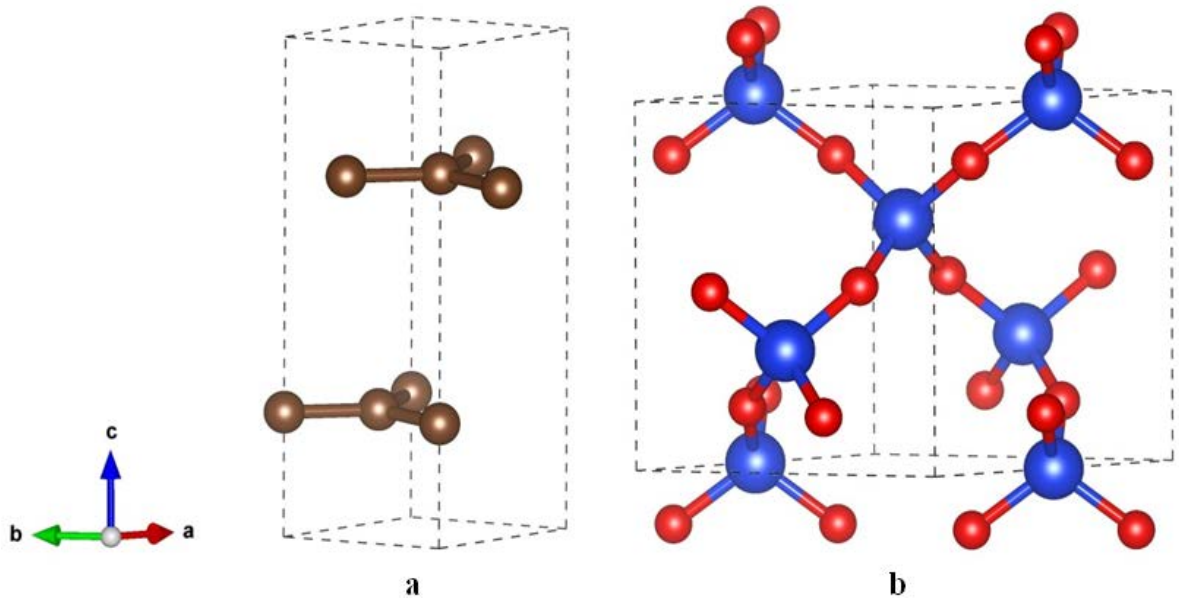

Fig. 1. Elementary cells of graphite-2H (a) and α-SiO_2 (b)

2. Computational details

The calculations were based on the density functional theory (DFT). All of calculations were carried out using VASP (Vienna *Ab initio* Simulation Package) [18-20]. The projector-augmented wave (PAW) potentials and Perdew–Burke–Ernzerhof (PBE) functional were used. The cutoff energy is of 520 eV. The valence electron configurations for Si, O, C, and H were [Ne] $3s^2 3p^2$, [He] $2s^2 2p^4$, [He] $2s^2 2p^2$ and $1s^1$, respectively. The atomic structures were relaxed until the forces on all unconstrained atoms were smaller than 0.01 eV/Å. A vacuum layer of 20 Å along *z* direction was constructed to eliminate the interaction with spurious replica images.

Table 1. Exchange-correlation functional for graphite-2H and α-SiO_2 structure calculation

Structure	Functional	Lattice constant			Difference with experiment, %
		a, Å	c, Å	c/a	
Graphite-2H	LDA[21]	2.4479	6.4596	2.6388	3.11
	PBE[22]	2.4692	7.5047	3.0393	11.59
	PBE-D2[23]	2.4647	6.3218	2.5649	5.82
	PBE-D3(zero)[24]	2.4682	6.7947	2.7529	1.08
	PBE-D3(BJ)[25]	2.4674	6.6772	2.7061	0.638
	Experiment[26]	2.4642	6.7114	2.7235	–
α-SiO_2 (quartz)	LDA[21]	5.0433	5.5341	1.0973	0.256
	PBE[22]	5.0038	5.5869	1.1165	1.490
	PBE-D2[23]	5.0886	5.5742	1.0954	0.428
	PBE-D3(zero)[24]	5.0867	5.5745	1.0959	0.385
	PBE-D3(BJ)[25]	5.0801	5.5704	1.0965	0.329
	Experiment[27]	4.9133	5.4053	1.1001	–

The calculations were carried out without spin polarization. The integration in reverse energy space was carried on the 7×7×7 and 5×5×5 *k*-points grids determined by a fine grid of gamma-centered method. The exchange-correlation functional chosen was based on the preliminary calculations of structural parameters of the graphite unit cells and α-SiO_2 and is given in Table 1.

The DFT-D3 method of Grimme demonstrated the smallest difference between the calculated and experimental magnitude of lattice constants and have been used for further calculation. Static self-consistent calculations were performed using the tetrahedron method and Bloch corrections. Integration in reverse energy space was carried on the 11×11×1 k-point grids. Structural figures and charge density drawings were produced by VESTA package [28].

3. Results and discussion

Figure 2 shows the positions of the graphene sheet with respect to the position of quartz unit cell. Ground states were found for each type of the surface and position of graphene sheets. The adsorption energy was calculated. The binding energy of carbon atoms in graphene with a substrate was determined on the basis of relation

$$E_{ads} = \frac{E_{total} - E_{gr} - E_{surf}}{n}, \quad (1)$$

where n is the number of graphene unit cells used in a supercell,

E_{total} is the total energy of graphene-SiO_2(0001) supercell,

E_{gr} is the total energy of graphene,

E_{surf} is the total energy of a quartz substrate.

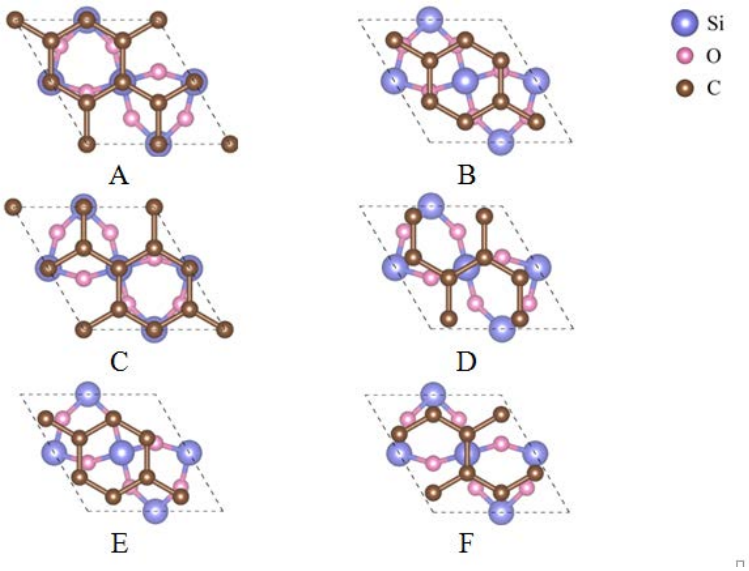

Fig. 2. Position of carbon atoms on quartz (0001) substrate

The interlayer distances and adsorption energy were calculated for all simulated structures (Figs. 3, 4). The absorption of graphene on the surface of quartz with oxygen dangling bonds is the most energetically favorable (E_{ads} = -281 meV). Binding energy between graphene and SiO_2 (0001) substrate is in range (-85 to -72.5 meV) for the other types of surface. Such binding energy indicates that there is physical adsorption of the graphene sheet on the quartz substrate surface.

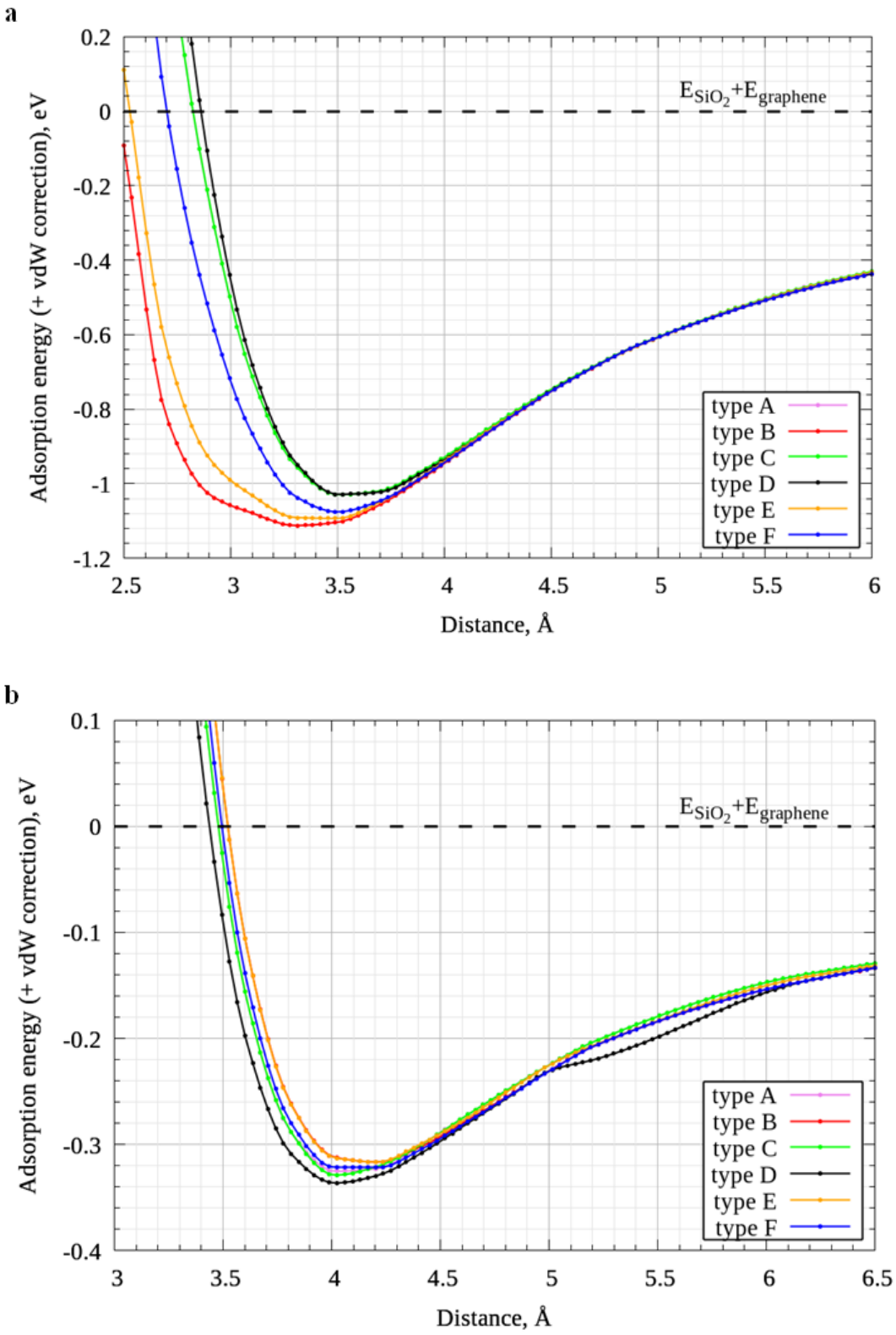

Fig. 3. Interlayer distances and adsorption energy of O^{sat}(a) and O^{unsat}(b) structures

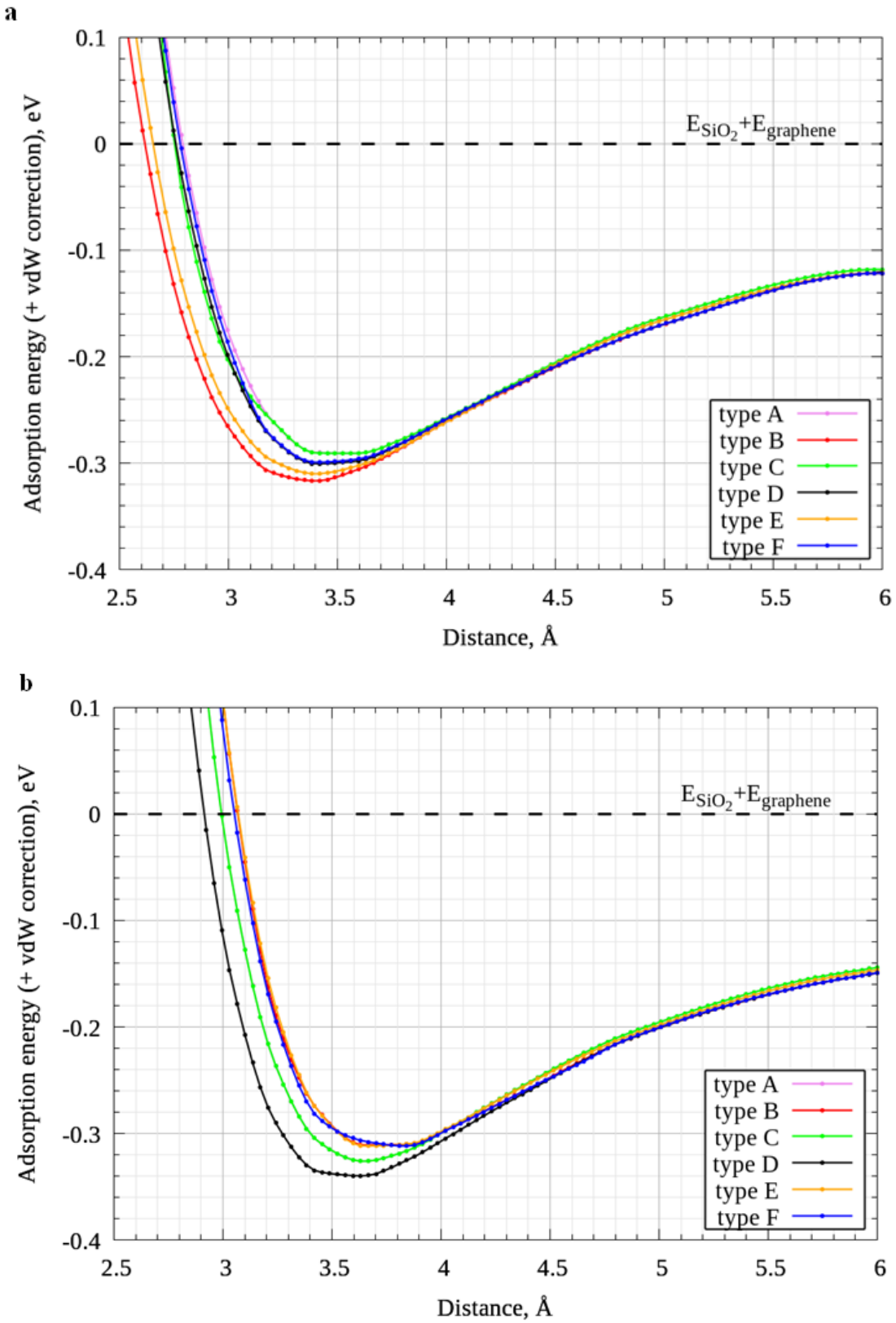

Fig. 4. Interlayer distances and adsorption energy of Si^{sat}(a) and Si^{unsat}(b) structures

Optimized structures of O^{unsat}, O^{sat}, Si^{unsat} and O^{sat} with adsorbed graphene sheet are shown in Fig. 5. The distances between the graphene layer and the substrate surface range from 3.31 to 4.32 Å that corresponds to physical adsorption with a strong influence of van der Waals forces.

Figure 6 shows charge densities for graphene on a quartz substrate. As seen from the figure, the nonequilibrium distribution of the graphene charge density is present near the O^{unsat} substrate. This can have a negative effect on the electronic properties of graphene.

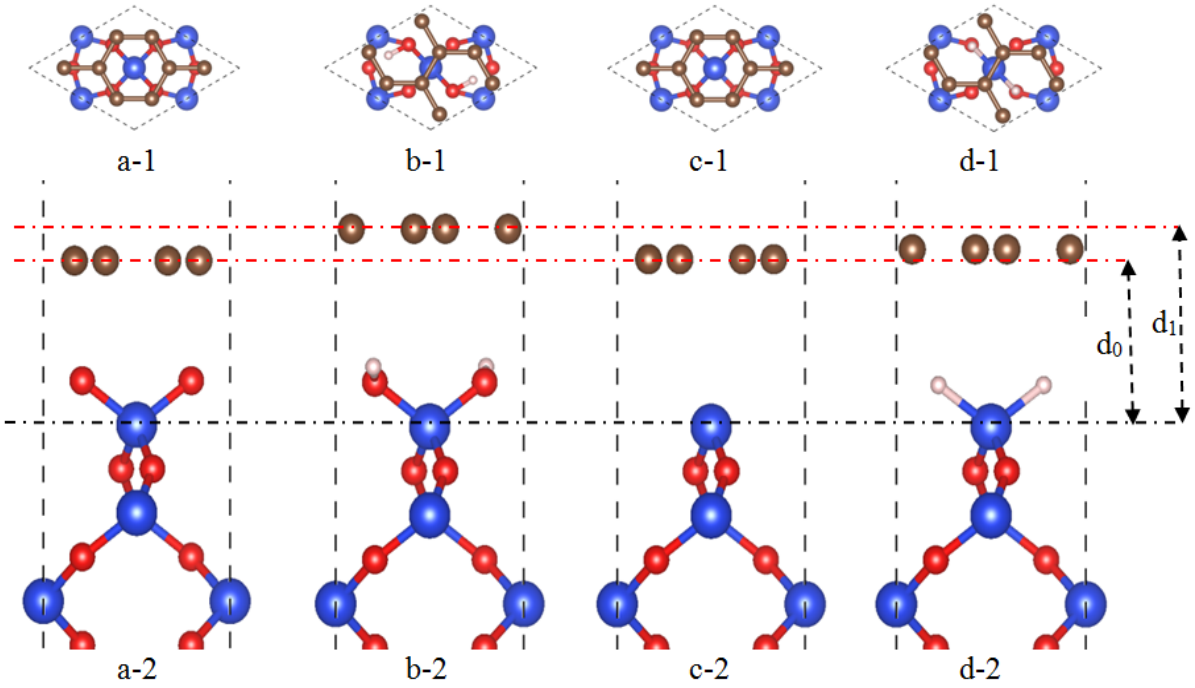

Fig. 5. Optimized structures of O^{unsat}, O^{sat}, Si^{unsat} and Si^{sat} with adsorbed graphene sheet

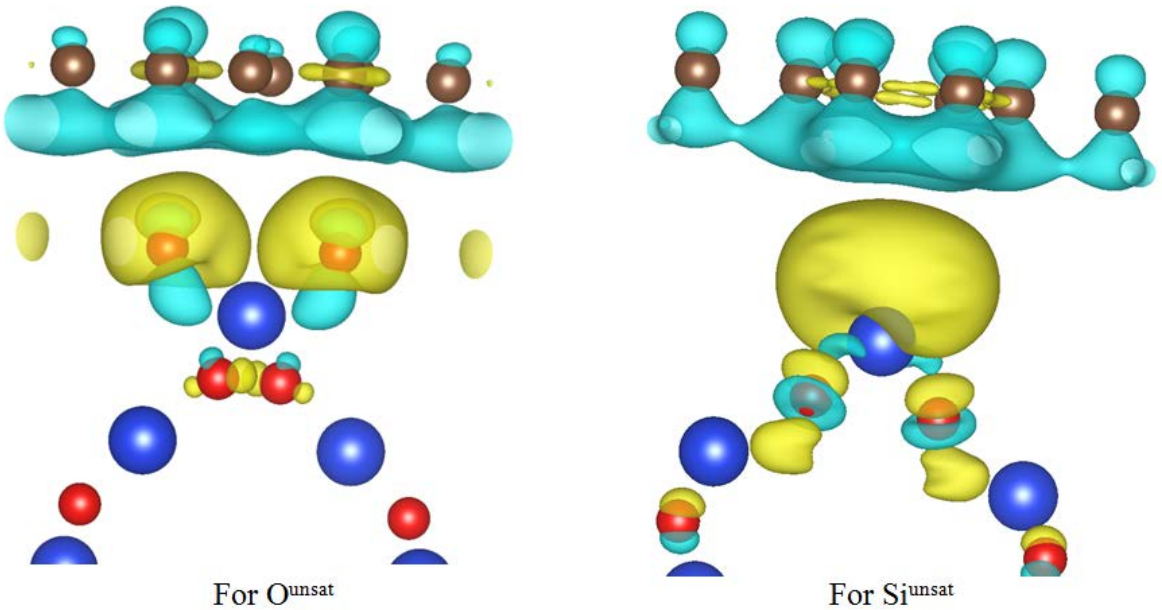

Fig. 6. Charge density of graphene on a quartz substrate

The band structures were calculated for the quartz substrate O^{unsat}, graphene and graphene on quartz. Changes in the states of graphene under the action of a substrate are observed in the immediate vicinity of the Fermi level. Energy gap arises width from 50 to 120 meV between the bonding and antibonding π-zones of graphene (Fig. 7).

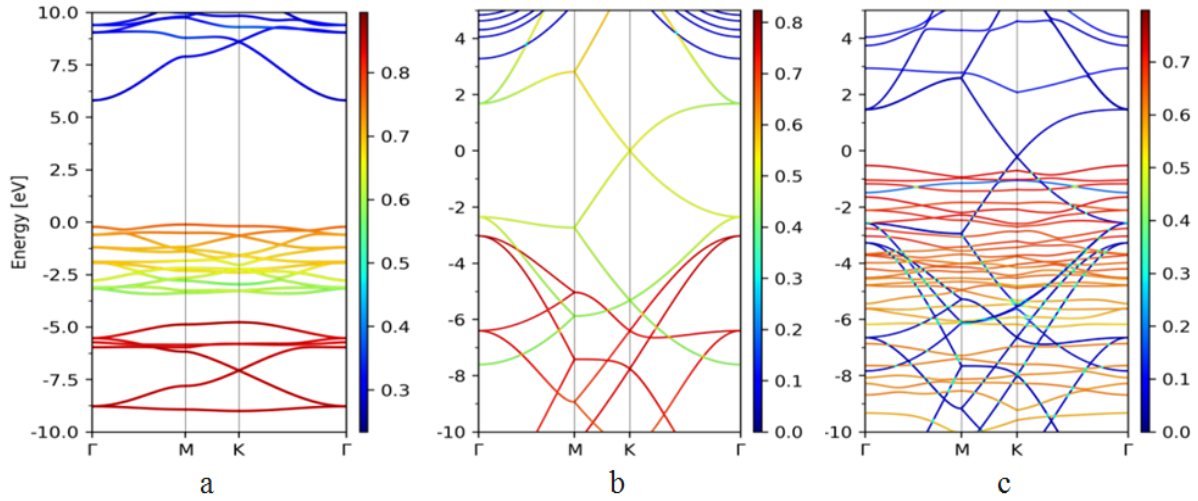

Fig. 7. Band structure of quartz (a), graphene (b) and graphene on quartz substrate (c)

4. Conclusions

The ground state of graphene position on the obtained SiO_2 surfaces has been determined. The interlayer distances between graphene and different types of quartz substrate have been calculated and are from 3.31 to 4.32 Å. It is found that the energy spectrum of graphene on substrate near the Fermi level is linear. The Fermi level is shifted toward to the valence band, which indicates a small redistribution of charge on the substrate. Overflow of charge occurs on the near-surface oxygen atoms (0.07 e/atom).The binding energy of 50 – 80 meV for the physical adsorption of graphene sheet on a quartz substrate. Electronic structure of adsorbed graphene has no changes.

Acknowledgements. *This work was supported by the grant 3.02 Belarusian National Scientific Research Program "Convergence 2020".*

References

[1] K. Geim, K.S. Novoselov, The rise of graphene // *Nat. Mater*. **6** (2007) 183.
[2] F. Schwierz, Graphene transistors // *Nat. Nanotechnol*. **5** (2010) 487.
[3] H. Castro Neto, F. Guinea, N.M.R. Peres, K.S. Novoselov, A.K. Geim, The electronic properties of graphene // *Rev. Mod. Phys*. **81** (2009) 109.
[4] J. Martin, N. Akerman, G. Ulbricht, T. Lohmann, J.H. Smet, K.V. Klitzing, A. Yacoby, Optical probing of electronic interaction between graphene and hexagonal boron nitride // *Nat. Phys*. **4** (2007) 144.
[5] Y. Zhang, V.W. Brar, C. Girit, M.F. Crommie, Origin of spatial charge inhomogeneity in graphene // *Nat. Phys*. **5** (2009) 722.
[6] A. Deshpande, W. Bao, Z. Zhao, C.N. Lau, B.J. LeRoy, Effect of charged impurity correlations on transport in monolayer and bilayer graphene // *Phys. Rev. B: Condens. Matter Mater. Phys*. **83** (2011) 155409.
[7] E.H. Hwang, S. Adam, S. Das Sarma, Carrier transport in two-dimensional graphene layers // *Phys. Rev. Lett*. **98** (2007) 186806.
[8] J.C. Meyer, A.K. Geim, M.I. Katsnelson, K.S. Novoselov, T.J. Booth, S. Roth, The structure of suspended graphene sheets // *Nature* **446** (2007) 60.
[9] M. Gibertini, A. Tomadin, F. Guinea, M.I. Katsnelson, M. Polini, Electron-hole puddles in the absence of charged impurities // *Phys. Rev. B: Condens. Matter Mater. Phys*. **85** (2012) 201405.

[10] M. Ishigami, J.H. Chen, W.G. Cullen, Atomic structure of graphene on SiO_2 // *Nano Lett.* **7** (2007) 1643.
[11] C.H. Lui, L. Liu, K.F. Mak, G.W. Flynn, T.F. Heinz, Ultraflat graphene // *Nature* **462** (2009) 339.
[12] J.H. Chen, C. Jang, S. Adam, M.S. Fuhrer, Correlated charged impurity scattering in graphene // *Nat. Phys*. **4** (2008) 377.
[13] A. Castellanos-Gomez, H.M. Smit, N. Agraıt, Spatially resolved electronic inhomogeneities of graphene due to subsurface charges // *Carbon* **50** (2012) 932.
[14] K.M. Burson, W.G. Cullen, S. Adam, C.R. Dean, K. Watanabe, T. Taniguchi, P. Kim, M.S. Fuhrer, Dependence of the energy transfer to graphene on the excitation energy // *Nano Lett*. **13** (2013) 3576.
[15] T.P.M. Goumans, A. Wander, W.A. Brown, C.R.A. Catlow, Structure and stability of the (001) α-quartz surface // *Chem. Phys*. **9** (2007) 2146.
[16] W. Steurer, A. Apfolter, M. Koch, T. Sarlat, E. Søndergard, W.E. Ernst, B. Holst, The structure of the α-quartz (0001) surface investigated using helium atom scattering and atomic force microscopy // *Surf. Sci*. **601** (2007) 4407.
[17] G-M. Rignanese, A. De Vita, J-C. Charlier, Density functional theory calculations on graphene/α-SiO_2(0001) interface // *Phys Rev B* **61** (2000) 13250.
[18] R.G. Parr, W. Yang, *Density-Functional Theory of Atoms and Molecules* (Oxford University Press, 1989).
[19] P.E. Blöchl, Projector augmented-wave method // *Phys. Rev. B: Condens. Matter Mater. Phys.* **50** (1994) 17953.
[20] G. Kresse, D. Joubert, From ultrasoft pseudopotentials to the projector augmented-wave method // *Phys. Rev. B: Mater. Phys*. **59** (1999) 1758.
[21] W. Kohn, L.J. Sham, Self-consistent equations including exchange and correlation effects // *Phys. Rev*. **140** (1965) A1133.
[22] J.P. Perdew, K. Burke, M. Ernzerhof, Generalized gradient approximation made simple // *Phys. Rev. Lett*. **77** (1996) 3865.
[23] S. Grimme, Semiempirical GGA-type density functional constructed with a long-range dispersion correction // *J. Comp. Chem*. **27** (2006) 1787.
[24] S. Grimme, J. Antony, S. Ehrlich, S. Krieg, A consistent and accurate ab initio parametrization of density functional dispersion correction (DFT-D) for the 94 elements H-Pu // *J. Chem. Phys*. **132** (2010) 154104.
[25] S. Grimme, S. Ehrlich, L. Goerigk, Effect of the damping function in dispersion corrected density functional theory // *J. Comp. Chem*. **32** (2011) 1456.
[26] http://www.handbookofmineralogy.org/pdfs/graphite.pdf
[27] G. Will, M. Bellotto, W. Parrish, M. Hart, Crystal structures of quartz and magnesium germanate by profile analysis of synchrotron-radiation high-resolution powder data // *J. Appl Cryst.* **21** (2000) 182.
[28] K. Momma, F. Izumi, VESTA 3 for three-dimensional visualization of crystal, volumetric and morphology data // *J. Appl. Crystallogr*. **44** (2011) 1272.